



## Ionic Liquid Electrolytes for Safer Lithium Batteries

### I. Investigation around Optimal Formulation

M. Moreno,<sup>a</sup> E. Simonetti,<sup>b</sup> G. B. Appetecchi,<sup>b,z</sup> M. Carewska,<sup>a</sup> M. Montanino,<sup>c</sup> G.-T. Kim,<sup>d,e</sup> N. Loeffler,<sup>d,e</sup> and S. Passerini<sup>d,e,\*</sup>

<sup>a</sup>ENEA (Agency for New Technologies, Energy and Sustainable Economic Development), DTE-PCU-SPCT, Rome 00123, Italy

<sup>b</sup>ENEA, SSPT-PROMAS-MATPRO, Rome 00123, Italy

<sup>c</sup>ENEA, SSPT-PROMAS-NANO, Portici 80055, Italy

<sup>d</sup>Helmholtz Institute Ulm - Karlsruhe Institute of Technology, 89081 Ulm, Germany

<sup>e</sup>Karlsruhe Institute of Technology (KIT), 76021 Karlsruhe, Germany

In this paper we report on the investigation of ionic liquid-based electrolytes with enhanced characteristics. In particular, we have studied ternary mixtures based on the lithium bis(trifluoromethanesulfonyl)imide (LiTFSI) salt and two ionic liquids sharing the same cation (*N*-methyl-*N*-propyl pyrrolidinium, PYR<sub>13</sub>), but different anions, bis(trifluoromethanesulfonyl)imide (TFSI) and bis(fluorosulfonyl)imide (FSI). The LiTFSI-PYR<sub>13</sub>TFSI-PYR<sub>13</sub>FSI mixtures, found to be ionically dissociated, exhibit better ion transport properties (about 10<sup>-3</sup> S cm<sup>-1</sup> at -20°C) with respect to similar ionic liquid electrolytes till reported in literature. An electrochemical stability window of 5 V is observed in carbon working electrodes. Preliminary battery tests confirm the good performance of these ternary electrolytes with high-voltage NMC cathodes and graphite anodes.

Ionic liquid electrolyte mixtures, PYR<sub>13</sub>TFSI, PYR<sub>13</sub>FSI.

© The Author(s) 2016. Published by ECS. This is an open access article distributed under the terms of the Creative Commons Attribution Non-Commercial No Derivatives 4.0 License (CC BY-NC-ND, <http://creativecommons.org/licenses/by-nc-nd/4.0/>), which permits non-commercial reuse, distribution, and reproduction in any medium, provided the original work is not changed in any way and is properly cited. For permission for commercial reuse, please email: [oa@electrochem.org](mailto:oa@electrochem.org). [DOI: 10.1149/2.0051701jes] All rights reserved.

Manuscript submitted August 2, 2016; revised manuscript received August 22, 2016. Published September 2, 2016. This was Paper 265 presented at the Chicago, Illinois, Meeting of the IMLB, June 19–24, 2016. *This paper is part of the Focus Issue of Selected Papers from IMLB 2016 with Invited Papers Celebrating 25 Years of Lithium Ion Batteries.*

Ionic liquids (ILs) are being investigated as substitutes of volatile and flammable organic electrolyte solvents in rechargeable lithium-ion battery systems<sup>1,2</sup> to enhance safety of the electrochemical device. ILs are considered, in fact, strong flame retardants, displaying negligible vapor pressure in combination with relatively fast ion transport properties and wide chemical/electrochemical/thermal stability.<sup>3,4</sup> So far, single ILs did not generally fully satisfy the requirements and/or operative conditions of practical devices, although their properties can be finely tuned by properly modifying their architecture.<sup>3,4</sup> A promising approach, however, is represented by suitably combining different ionic liquids, leading to beneficial synergic effects on the physicochemical properties of the resulting mixtures.<sup>5-7</sup>

In previous work,<sup>8,9</sup> we have demonstrated the possibility of favorably combining two ionic liquids, sharing the *N*-methyl-*N*-propyl pyrrolidinium cation (PYR<sub>13</sub><sup>+</sup>) and bis (trifluoromethanesulfonyl)imide (TFSI<sup>-</sup>) and bis(fluorosulfonyl)imide (FSI<sup>-</sup>) anions. The TFSI ion was proved to be stable toward oxidation and thermally robust<sup>2</sup> while FSI-based ILs exhibit good ion conduction even at low temperature and protective film-forming capability onto electrodes.<sup>2,10,11</sup> In particular, proper PYR<sub>13</sub>TFSI-PYR<sub>13</sub>FSI formulations<sup>8,9</sup> were found to display ionic conductivities largely overcoming 10<sup>-4</sup> S cm<sup>-1</sup> at -20°C whereas the pure IL materials, still in solid state, exhibit conduction values about four orders of magnitude lower. This behavior is likely due to the different hindrance of the anions, resulting in worse ion packing and, therefore, inhibiting the crystallization process of the IL blend.<sup>5-7</sup> In addition, average, even if moderate, variation of the linear density vs mole composition behavior of the PYR<sub>13</sub>TFSI-PYR<sub>13</sub>FSI mixtures was observed at intermediate FSI mole fraction.<sup>9</sup> This issue suggests rearrangement of the ion structural organization within the IL blend, which may positively reflect on the transport properties. On the basis of the obtained results, the TFSI:FSI mole ratio of 2:3 was selected.<sup>9</sup>

In the present work, we have prepared ternary mixtures by incorporating different fractions of the LiTFSI salt into the PYR<sub>13</sub>TFSI-PYR<sub>13</sub>FSI blend, having care to keep the overall TFSI:FSI mole ratio = 2:3. The physicochemical and electrochemical properties of the resulting LiTFSI-PYR<sub>13</sub>TFSI-PYR<sub>13</sub>FSI electrolytes were studied. Finally, preliminary battery tests with NMC cathodes and graphite anodes were performed.

### Experimental

**Preparation of ternary electrolytes.**—The PYR<sub>13</sub>TFSI ionic liquid was synthesized through a procedure described in details elsewhere.<sup>12</sup> The chemicals *N*-methylpyrrolidine (97 wt%), 1-bromopropane (99 wt%), activated charcoal (Aldrich, Darco-G60) and alumina (acidic, Aldrich Brockmann I) were purchased by Aldrich and, as well as lithium bis(trifluoromethanesulfonyl)imide, LiTFSI (99.9 wt%, battery grade) purchased by 3 M, used as received. PYR<sub>13</sub>FSI (99.9 wt%) was purchased by Solvionic and vacuum dried at 70°C for three days. Deionized H<sub>2</sub>O was obtained with a Millipore ion-exchange resin deionizer.

The water content was measured by an automatic Karl Fischer coulometer titrator (Mettler Toledo DL32) inside the dry room (R.H. < 0.1% at 20°C). The Karl Fischer titrant was one-component reagent (Hydranal 34836 Coulomat AG) purchased from Aldrich.

The ternary electrolyte mixtures were prepared in the dry room by dissolving (at 40–50°C for 10–15 minutes) the proper amount of LiTFSI (previously vacuum dried at 120°C overnight) in the suitable PYR<sub>13</sub>TFSI-PYR<sub>13</sub>FSI blend. The IL samples were stored in vacuum desiccator within the dry room.

**Density measurements.**—The density measurements were carried out (inside the dry room) within the 20–90°C temperature range by running a cooling scan at 10°C steps with a density meter (Mettler Toledo DE40). Prior the measurements, the electrolyte samples were vacuum degassed at 50°C for at least 18 hours to prevent bubble formation (during the cooling scan).

\*Electrochemical Society Member.

<sup>z</sup>E-mail: [gianni.appetecchi@enea.it](mailto:gianni.appetecchi@enea.it)

**Viscosity measurements.**—The rheological properties were investigated using a rheometer (HAAKE RheoStress 600) located in the dry room. The measurements were carried out (within a rotation speed range from 100 to 2000  $\text{s}^{-1}$ ) by running a heating scan at  $10^\circ\text{C}$  steps ( $1^\circ\text{C min}^{-1}$ ) from 20 to  $80^\circ\text{C}$ .

**Ionic conductivity.**—The ion conduction values of the ionic liquid electrolyte mixtures were determined by impedance spectroscopy measurements performed with a Frequency Response Analyzer (Schlumberger Solartron mod. 1260) on symmetrical two-electrode cells. A voltage amplitude ( $\Delta V$ ) equal to 10 mV, within the frequency range from 100 kHz to 1 Hz, was applied. The ILs were housed (within the dry room) in sealed, glass cells (AMEL 192/K1) equipped with two porous platinum electrodes (cell constant ranging from 0.90 to 1.10 cm with an error equal to  $\pm 0.01 \text{ cm}^{-1}$ ). The AC measurements were run in the  $-40$  to  $100^\circ\text{C}$  temperature range by using a climatic chamber (Binder GmbH MK53). To completely crystallize the ionic liquid samples,<sup>13</sup> the cells were immersed in liquid nitrogen for a few seconds and, then, transferred into the climatic chamber at  $-40^\circ\text{C}$ . After a few minutes of storage at this temperature, the solid samples turned again molten. This protocol was repeated until the IL samples remained solid at  $-40^\circ\text{C}$ . Successively, the cells were held at  $-40^\circ\text{C}$  overnight and, finally, were subjected to a heating scan at  $1^\circ\text{C h}^{-1}$ . Ionic conductivity measurements as well as all electrochemical tests were carried out in the dry room.

**Electrochemical stability.**—The electrochemical stability of the ternary ionic liquid mixtures was evaluated by linear sweep (LSVs) and cyclic (CVs) voltammetries run on lithium metal (counter and reference electrode)/IL sample/carbon (working electrode) vacuum-sealed, pouch-cells manufactured in the dry room. The working electrode was prepared blending Super C45 (IMERYs, 80% in weight) carbon black and sodium-carboxymethylcellulose (CMC, Dow Wolff Cellulosics) binder in water. The so-obtained slurry was cast onto aluminum (anodic LSVs) or copper (cathodic CVs) foils. The solvent removal was initially allowed at room temperature and, then, under vacuum at  $170^\circ\text{C}$  overnight. Discs of 12 mm diameter (corresponding to a geometrical area equal to  $1.13 \text{ cm}^2$ ) were punched from the carbon electrode tapes. Separate tests were carried out on each sample to determine the anodic (by LSVs) and cathodic (CVs) electrochemical stability limits. The measurements were carried out scanning the cell voltage from the OCV value towards: *a*) more positive (anodic limit) voltages (LSVs); *b*) more negative (cathodic limit) voltages and, successively, running consecutive cyclic voltammetries between  $-0.3 \text{ V}$  (vs  $\text{Li/Li}^+$ ) and  $0.5 \text{ V}$  (CVs). Clean electrodes and fresh cells were used for each test. To confirm the reproducibility of the results, the LSV tests were run at least twice on different fresh cells. The measurements were performed at  $20^\circ\text{C}$  using a VMP3 (Bio-Logic SAS) galvanostat/potentiostat.

**Tests in battery.**—The battery performance of the  $\text{LiTFSI-PYR}_{13}\text{TFSI-PYR}_{13}\text{FSI}$  electrolyte systems was preliminary evaluated in  $\text{Li/NMC}$  and  $\text{Li/graphite}$  pouch cells. Cathode and anode tapes<sup>14</sup> were prepared by respectively blending: *i*)  $\text{LiNi}_{0.33}\text{Mn}_{0.33}\text{Co}_{0.33}\text{O}_2$  (NMC, TODA, 88 wt%), sodium-carboxymethylcellulose (CMC, Dow Wolff Cellulosics, 5 wt%) and carbon black (Super C45, IMERYs, 7 wt%); *ii*) graphite (SLP 30, IMERYs, 91 wt%), CMC (5 wt%) and carbon black (4 wt%). The lithium cells were manufactured (within the dry room) by laminating together a lithium foil (50  $\mu\text{m}$ ), a polymer separator (Asahi Kasei, Hipore SV718) and a NMC (or graphite) electrode, which were then housed within soft envelopes. The IL electrolyte was previously loaded into the separator. Successively, the envelopes (previously evacuated for 30 minutes) were vacuum-sealed.

The cells were investigated through galvanostatic cycling measurements performed by a Maccor 4000 battery cyler. The tests were run at 0.1 C and  $23^\circ\text{C}$  (controlled by climatic chamber) within the 3.0 – 4.3 (vs  $\text{Li/Li}^+$ ) and 0.01 – 2.0 V voltage ranges for the  $\text{Li/NMC}$  and  $\text{Li/graphite}$  cells, respectively. A potentiostatic step, e.g., apply-

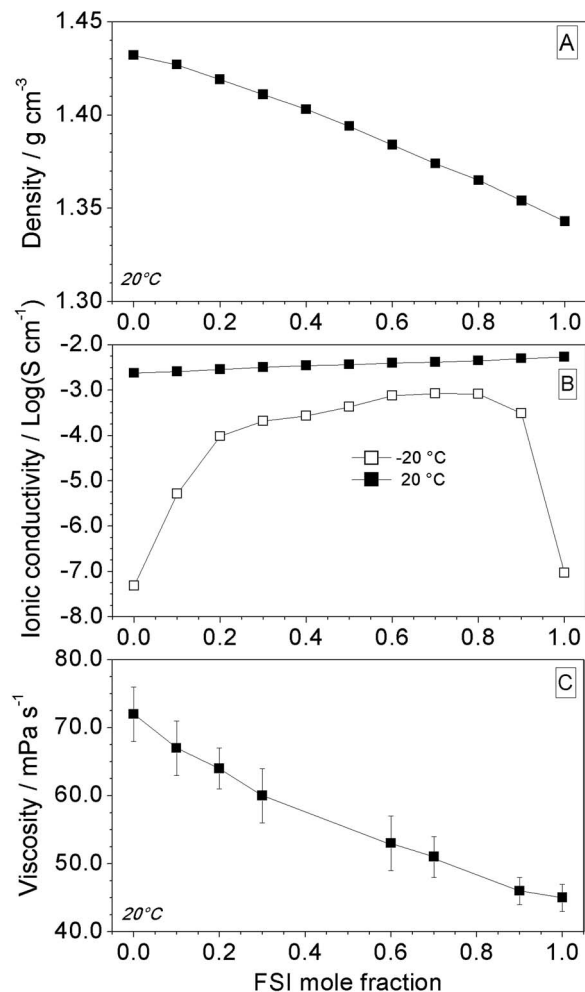


**Figure 1.** Density (panel A), ionic conductivity (panel B) and viscosity (panel C) vs. FSI mole fraction dependence of  $\text{PYR}_{13}\text{TFSI-PYR}_{13}\text{FSI}$  binary ionic liquid mixtures at  $20^\circ\text{C}$ . The conductivity data are reported also at  $-20^\circ\text{C}$ . The error bars fall within the data markers. Data from reference 9.

ing a 0.01 V voltage until the residual current decays down to 1/10 of the nominal value, was run upon each discharge half-cycle for the  $\text{Li/graphite}$  cells in order to promote full lithium intercalation.

## Results and Discussion

The aqueous procedure route allowed to synthesize high purity ( $\text{Li}^+$  and  $\text{Br}^-$  content below 2 ppm), anhydrous, clear, colorless and odorless ionic liquid samples with yields ranging from 85 to 90 mol.%. Ternary electrolyte mixtures with water content below 2 ppm were prepared.

Figure 1 summarizes the physicochemical characteristics of  $\text{PYR}_{13}\text{TFSI-PYR}_{13}\text{FSI}$  binary blends,<sup>9</sup> prepared in order to synergistically combining two different ionic liquids. The results, coming from previous investigation,<sup>9</sup> show how at low temperatures ( $\leq -20^\circ\text{C}$ ) proper formulations of the ionic liquid mixtures exhibit extremely higher conductivity values with respect to the single materials which, conversely, are in the solid state ( $\text{PYR}_{13}\text{TFSI}$  and  $\text{PYR}_{13}\text{FSI}$  melt at 12 and  $-9^\circ\text{C}$ , respectively).<sup>2</sup> This behavior, in good agreement with the DSC results previously reported,<sup>9</sup> is due to the different steric hindrance of the TFSI and FSI anions, which hinders the crystallization of the ionic liquid mixtures.<sup>2,9</sup> Nevertheless, above  $0^\circ\text{C}$ , e.g., where the mixtures as well as the single ILs are in the molten state, the ion conduction is seen to increase with increasing the content of the more conductive ionic liquid ( $\text{PYR}_{13}\text{FSI}$ ). The FSI mole fraction was chosen equal to 0.6 as the right compromise among fast ion transport

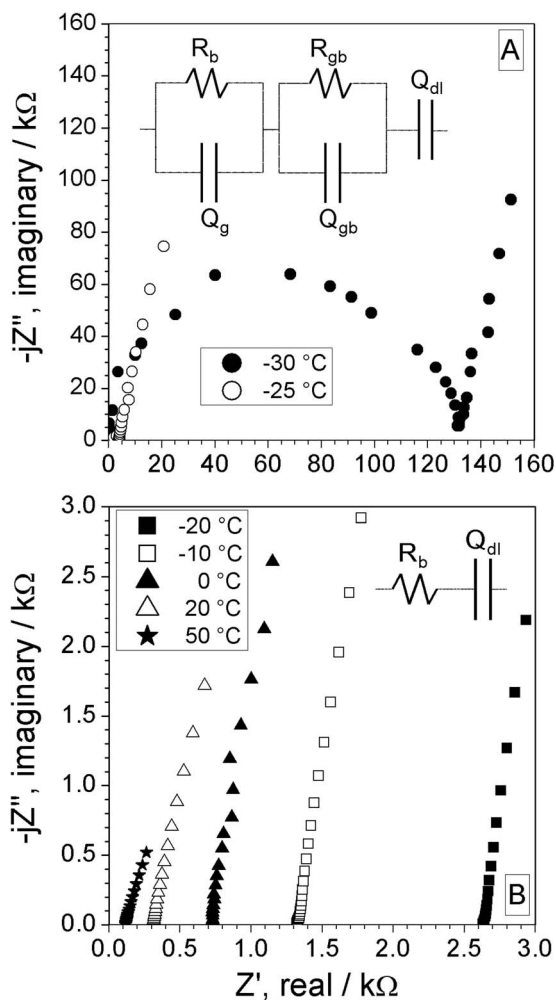


**Figure 2.** Impedance plots taken on a symmetrical Pt/0.1LiTFSI-0.3PYR<sub>13</sub>TFSI-0.6PYR<sub>13</sub>FSI/Pt cell at selected temperatures. Frequency range: 65 kHz – 1 Hz. Panel A: from –30 to –25°C. Panel B: from –20 to 50°C. The equivalent circuit models using for fitting the AC responses are reported as inserts in panels A and B.

properties even at low temperatures, electrochemical/thermal stability, good film-forming ability and cost (FSI is rather expensive). This corresponds to a FSI/TFSI mole ratio equal to 3:2. Therefore, the (x)LiTFSI-(y)PYR<sub>13</sub>TFSI-(1-x-y)PYR<sub>13</sub>FSI (where x, y and (1-x-y) represent the mole fraction of the single components, respectively) ternary ionic liquid mixtures were prepared having care to keep the overall FSI mole fraction (1-x-y) equal to 0.6. The LiTFSI mole fraction was ranged from 0 to 0.2, corresponding to a molar concentration from 0 M to 1.12 M.

The ternary electrolytes were subjected to impedance measurements aiming to determinate the ionic conductivity behavior. As example, Figure 2 illustrates selected AC plots obtained at various temperatures during the heating scans carried out on the 0.1LiTFSI-0.3PYR<sub>13</sub>TFSI-0.6PYR<sub>13</sub>FSI sample. At low temperatures (–30°C), the IL mixture exhibits the typical impedance response of an electrolyte sandwiched between two quasi-blocking electrodes.<sup>15</sup> A high frequency (100–1 kHz) semicircle is observed (falling into the origin of the axes), which was seen to be associated to two different contributes, i.e., bulk and grain boundary electrolyte resistance<sup>15</sup> as confirmed by the analysis of the AC measurements, suggesting the presence of heterogeneous phases within the IL sample. At lower frequencies (<1 kHz), an inclined straight line toward the real axes (Z'), typical of the blocking electrode capacitive behavior,<sup>15</sup> is displayed. At slightly higher temperatures (from –30 to –25°C), the semicircle

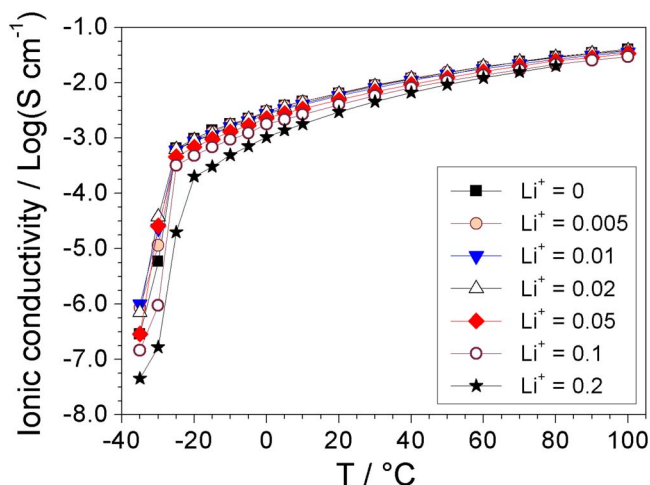


**Figure 3.** Conductivity vs. temperature dependence of (x)LiTFSI-(y)PYR<sub>13</sub>TFSI-(1-x-y)PYR<sub>13</sub>FSI ternary ionic liquid mixtures at different Li<sup>+</sup> mole fractions. The FSI/TFSI mole ratio was kept equal to 3:2. The error bars fall within the data markers.

is remarkably reduces (poorly visible in panel A) and shifted to higher frequencies due to the electrolyte resistance decrease with the temperature raise.<sup>15</sup> It is interesting to note that the response feature change in passing from –30 to –25°C (e.g., progressively disappearance of the semicircle) indicates minimization of the grain boundary contribution and increase in ionic conductivity. At –20°C (panel B) just an inclined straight-line, whose intercept with the real axes gives the IL electrolyte sample ionic resistance,<sup>15</sup> is seen in the AC plots. Further increase in temperature (>–20°C) results in progressive shift of the high frequency intercept toward lower resistance values and no spectrum shape change was noticed up to 100°C.

The analysis of the impedance responses was performed defining an equivalent circuit model taking into account all possible contributes to the impedance of the electrolyte under test.<sup>15</sup> The validity of the chosen circuit was confirmed by fitting the AC responses using a Non-Linear Least-Square (NLLSQ) software developed by Boukamp,<sup>16,17</sup> only fits characterized by a  $\chi^2$  factor<sup>16,17</sup> lower than  $10^{-4}$  were considerable acceptable. The general equivalent circuit (see insert in Figure 2A), proposed to represent the electrochemical cell under study (i.e., Pt / IL sample / Pt), takes into account both the bulk ( $R_b$ ) and the grain boundary ( $R_{gb}$ ) contributes to the total resistance of the IL electrolyte mixture. A constant-phase element, CPE (Q), was used in the place of pure capacitance (C). The  $Q_g$  and  $Q_{gb}$  (in parallel with  $R_b$  and  $R_{gb}$ , respectively) elements are related to the geometric and the grain boundary capacitance, respectively. Finally, the  $Q_{dl}$  element takes into account the double layer capacitance at electrolyte/electrode interface. Above –20°C, due to substantial modification of the shape of the AC plots, the impedance responses can be properly fitted by a simplified version of the equivalent circuit (see insert in Figure 2B), i.e., formed by the  $R_b$  (bulk resistance) and  $Q_{dl}$  (double layer capacitance) elements connected in series.

The transport properties of the ternary IL mixtures were investigated in terms of conductivity vs temperature dependence as in Figure 3. From –40 to about –25°C a linear rise from  $10^{-7}$  to above  $10^{-4}$  S cm<sup>-1</sup> was observed, indicating progressively enhanced ion mobility even if the samples are still in solid phase, likely due to solid-solid phase transitions. Around –25°C the conductivity vs temperature slope substantially changes, due to melting of the ionic liquid blends, in agreement with DSC results.<sup>9</sup> In the molten state (>–20°C) a progressively increasing slope is displayed, typical of VTF behavior.<sup>5-7</sup> Around  $10^{-3}$  S cm<sup>-1</sup> and  $10^{-2}$  S cm<sup>-1</sup> are already approached at –20°C and 40°C, respectively, representing ones of the best, if not the best, ion conduction values till reported in literature for ionic liquid electrolyte mixtures.<sup>2,18</sup>

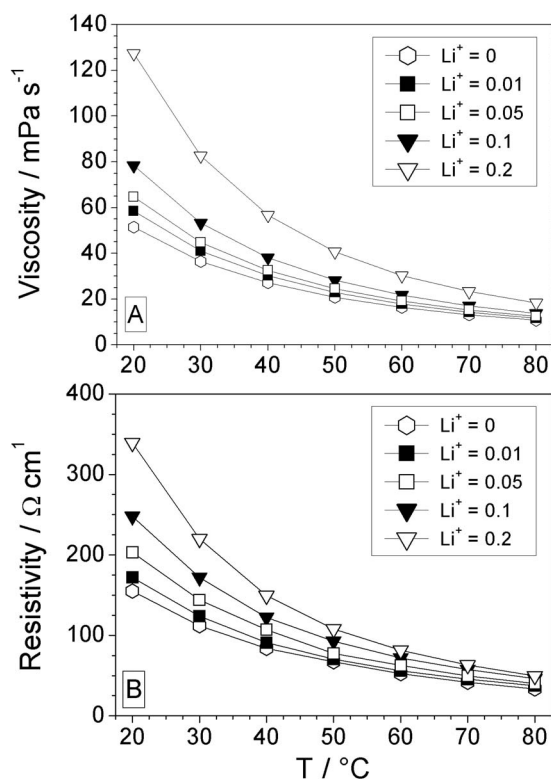


**Figure 4.** Viscosity (panel A) and resistivity (panel B) vs. temperature dependence of (x)LiTFSI-(y)PYR<sub>13</sub>TFSI-(1-x-y)PYR<sub>13</sub>FSI ternary ionic liquid mixtures at different Li<sup>+</sup> mole fractions. The FSI/TFSI mole ratio was kept equal to 3:2. The error bars fall within the data markers.

The addition of LiTFSI salt (regarded as replacement of pyrrolidinium cations with Li<sup>+</sup> ones) is seen further hindering crystallization of the IL mixtures, highlighted by a shift of the conductivity behavior slope change (toward lower temperatures) with respect to the LiTFSI-free sample (in agreement with the thermal measurements).<sup>9</sup> This results from unfavorable ion packing ascribable to the different size of the Li<sup>+</sup> and (PYR<sub>13</sub>)<sup>+</sup> cations,<sup>10,13</sup> able to counterbalance the stronger cation . . . anion interactions (e.g., due to the higher charge surface density of the smaller Li<sup>+</sup> cation with respect to the PYR<sub>13</sub><sup>+</sup> ones) which, conversely, lead to an increase of the melting temperature. No relevant shift of the conductivity vs temperature knee is observed with increasing the LiTFSI content (once more agreeing the DSC results),<sup>9</sup> suggesting that higher lithium salt concentrations do not substantially affect the melting temperature of the IL mixtures. At the same time, LiTFSI incorporation results in progressive conductivity decrease of the molten samples, ascribable to the increasing viscous drag deriving from the enhanced ion interactions,<sup>13,19</sup> confirmed by the rheological measurements depicted in Figure 4. However, a bell behavior is observed at very low temperatures ( $\leq -25^\circ\text{C}$ ). At lower LiTFSI mole fractions ( $<0.05$ ) the increase of the lithium salt content leads to conductivity raise (from one to two orders of magnitude) as a result of the melting temperature decrease. Conversely, at higher mole fractions ( $>0.05$ ) further addition of LiTFSI results in ion conduction decay due to remarkable viscosity increase (especially at low temperatures).

Rheological measurements were performed to better understand the conduction phenomena. Figure 4 plots the dependence of the viscosity (panel A) and resistivity (panel B, for comparison purpose) vs temperature. The measurements were run from 20 up to 80°C, e.g., where the IL mixtures show Newtonian behavior. From Figure 4 it is clearly evident how the viscosity and resistivity (inverse of conductivity) exhibit identical behavior, e.g., a continuous decrease is observed with increasing the temperature as well as a progressive increase is seen with raising the lithium salt content, once more resulting

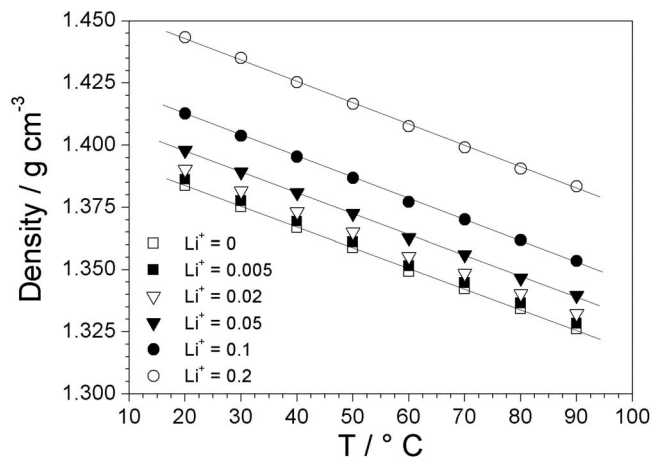


**Figure 5.** Density vs. temperature dependence of (x)LiTFSI-(y)PYR<sub>13</sub>TFSI-(1-x-y)PYR<sub>13</sub>FSI ternary ionic liquid mixtures at different Li<sup>+</sup> mole fractions. The FSI/TFSI mole ratio was fixed equal to 3:2. The error bars fall within the data markers.

in stronger and stronger ion interactions (due to Li<sup>+</sup>). Therefore, the ion transport properties of the LiTFSI-PYR<sub>13</sub>TFSI-PYR<sub>13</sub>FSI ternary mixtures appear well correlated with the rheological ones, i.e., the ion movement is mostly affected by the viscous drag.<sup>20,21</sup>

The physicochemical properties of the LiTFSI-PYR<sub>13</sub>TFSI-PYR<sub>13</sub>FSI electrolyte system were also investigated in terms of density at different temperatures as reported in Figure 5. The ternary mixtures (in the molten state), exhibiting a lithium salt concentration ranging from 0 to 1.12 M, differ in density of less than 4% within the investigated temperature range (i.e., 20–90°C). A linear decrease with the temperature raise is observed, displaying identical slope not dependently on the LiTFSI content. Also, a density increase is observed with increasing the Li<sup>+</sup> mole fraction. Such a behavior, already detected in other IL blends,<sup>7</sup> might suggest structural organizational rearrangement of the cations (Li<sup>+</sup>, PYR<sub>13</sub><sup>+</sup>) and anions (TFSI<sup>-</sup>, FSI<sup>-</sup>) within the mixtures, leading to different ion packing with increasing the lithium salt content. However, further work is required to confirm this hypothesis.

A qualitative estimation of the ion dissociation of the LiTFSI-PYR<sub>13</sub>TFSI-PYR<sub>13</sub>FSI mixtures was obtained by the Walden rule<sup>22–24</sup>

$$\Lambda \eta = k \quad [1]$$

which correlates the molar conductivity ( $\Lambda$ ) and the viscosity ( $\eta$ ) through a temperature dependent constant ( $k$ ) as reported in Figure 6. The dotted straight line, e.g., a 0.01 N KCl aqueous solution known for being fully dissociated and having ions of equal mobility,<sup>22</sup> is used as the calibration curve (ideal Walden line). The LiTFSI-PYR<sub>13</sub>FSI-PYR<sub>13</sub>TFSI samples are seen to lie just below the ideal line of the diagram, independently on the Li<sup>+</sup> mole fraction and temperature. This behavior, corresponding to the most favorable conditions for ionic liquids<sup>22</sup> as high conductivity is combined with low viscosity, suggests that the ternary mixtures are mostly consist of independently mobile ions.<sup>23</sup> Therefore, the LiTFSI-PYR<sub>13</sub>FSI-PYR<sub>13</sub>TFSI system might be modeled as a quasi-ideal lattice, in which positive charges are almost uniformly distributed around the negative ones.<sup>25–27</sup> In addition, neither the Li<sup>+</sup> content, nor the temperature are found to affect the “ionicity” of the LiTFSI-PYR<sub>13</sub>TFSI-PYR<sub>13</sub>FSI ternary electrolyte mixtures.

The electrochemical stability plays a key role in defining the average operative voltage range of electrolytes in battery systems. Therefore, this crucial parameter was evaluated toward carbon working electrodes aiming to obtain more reliable results. For instance, overestimation of the electrochemical stability is generally observed in (smooth) inert electrodes (platinum, nickel, stainless steel) whereas the large surface area of carbon (rich of active sites) electrodes allows of better simulating the behavior of electrolytes in average battery systems.

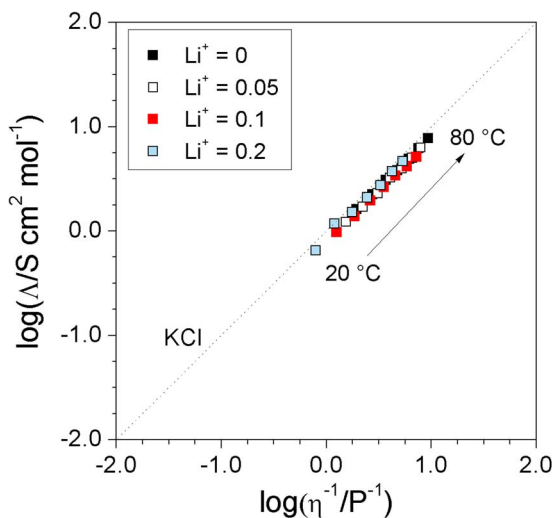


**Figure 6.** Walden plot of (x)LiTFSI-(y)PYR<sub>13</sub>TFSI-(1-x-y)PYR<sub>13</sub>FSI ternary ionic liquid mixtures. The dotted straight line, due to a 0.01 N KCl solution, fixes the position of the ideal Walden line.

Figure 7 reports the results coming from anodic and cathodic sweep voltammeteries performed on selected LiTFSI-PYR<sub>13</sub>TFSI-PYR<sub>13</sub>FSI mixtures at different Li<sup>+</sup> mole fraction. All potentials are given vs the Li/Li<sup>+</sup> redox couple. The addition of lithium salt (blue and red traces) results in progressive increase of the current density above 4 V (not observed in the LiTFSI-free mixture), even if somewhat low values, e.g., below 30 μA cm<sup>-2</sup>, of the residual current flow are detected up to 4.5 V. This issue was likely addressed to impurities, deriving from LiTFSI, able to catalyze the oxidation of the anions (TFSI and FSI). Repeated cyclic voltammeteries (reported in panel A of Figure 8), run on Li / 0.1LiTFSI-0.3PYR<sub>13</sub>TFSI-0.6PYR<sub>13</sub>FSI / carbon cells within the 3.0–5.0 V voltage range, have evidenced sharp reduction of the residual current density flow (down to just a few μA cm<sup>-2</sup> up to 4.5 V) even upon the first cycle. This clearly indicates irreversibility of the oxidation processes taking place during the first anodic scan in conjunction with very rapid consumption of impurities, therefore supporting for good stability of the LiTFSI-PYR<sub>13</sub>TFSI-PYR<sub>13</sub>FSI electrolyte mixtures toward oxidation up to 4.5 V. It is worth to note that no corrosion phenomenon is observed in Figure 8A, despite the TFSI and, especially, FSI anions were found to be a little bit corrosive for aluminum substrate.<sup>28–29</sup> However, this behavior could be related to the impurity

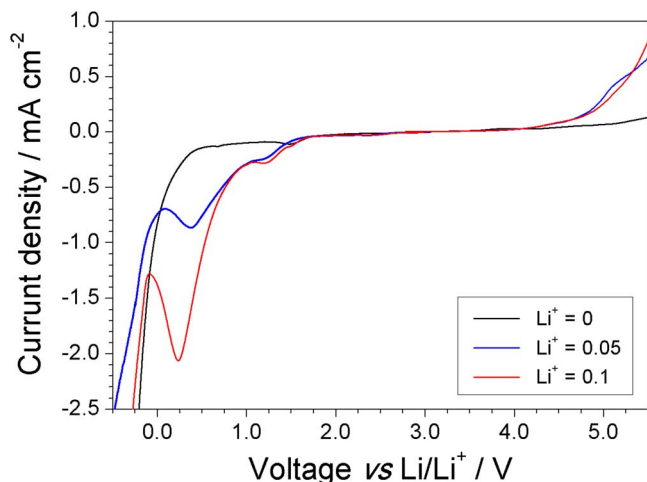


**Figure 7.** Linear sweep voltammetry of selected (x)LiTFSI-(y)PYR<sub>13</sub>TFSI-(1-x-y)PYR<sub>13</sub>FSI ternary ionic liquid mixtures at 20 °C. Carbon as the working electrode. Lithium as the counter and reference electrode. Scan rate: 5 mV s<sup>-1</sup>.

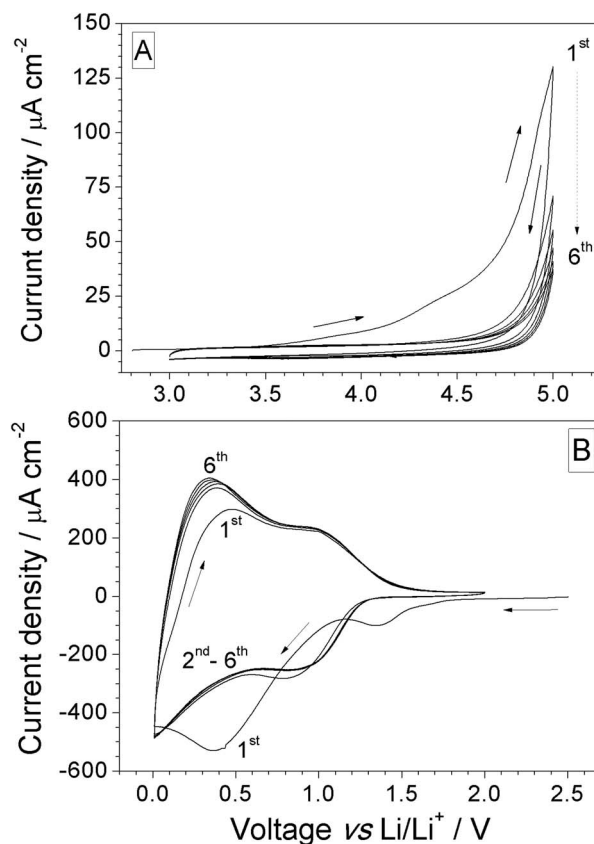


**Figure 8.** Anodic (panel A) and cathodic (panel B) cyclic voltammeteries of the (0.1)LiTFSI-(0.3)PYR<sub>13</sub>TFSI-(0.6)PYR<sub>13</sub>FSI sample at 20 °C. Carbon as the working electrode. Lithium as the counter and reference electrodes. Scan rate: 1 mV s<sup>-1</sup>.

and moisture content within the ionic liquid electrolyte (for instance, the LiTFSI-PYR<sub>13</sub>TFSI-PYR<sub>13</sub>FSI mixtures exhibit very low impurity and moisture content). In addition, the (working) carbon electrode may protect the Al substrate toward the ionic liquid electrolyte.

On the cathodic side (Figure 7), two features, e.g., around 1.25 and 0.3 V vs Li/Li<sup>+</sup>, are observed, likely ascribable to SEI formation and lithium intercalation into the carbon working electrode, respectively. The feature detected about 0.3 V, missing (as expected) in the LiTFSI-free sample (black trace), is seen to remarkably increase in passing from a lithium salt mole fraction equal to 0.05 to 0.1, resulting from intercalation of larger Li<sup>+</sup> amount. Below 0 V (vs Li/Li<sup>+</sup>) massive reduction of electrolyte (mainly pyrrolidinium cation) takes place. Consecutive cyclic voltammeteries (panel B of Figure 8), once more carried out on Li / 0.1LiTFSI-0.3PYR<sub>13</sub>TFSI-0.6PYR<sub>13</sub>FSI / carbon cells within 0.01–2.0 V, have shown well-defined reproducible current vs voltage profiles and, therefore, the possibility to reversibly intercalate lithium cations in these ionic liquid mixture with good efficiency and without any appreciable electrolyte degradation. The disappearance of the cathodic feature around 1.3 V (vs Li/Li<sup>+</sup>) upon the first cycle suggests establishment of suitable SEI onto the carbon working electrode (allowing reversible Li<sup>+</sup> intercalation process). Therefore, on the basis of the results obtained from voltammetric tests, the sample 0.1LiTFSI-0.3PYR<sub>13</sub>TFSI-0.6PYR<sub>13</sub>FSI is found to exhibit an average electrochemical stability window (ESW) of about 5 V, equal or wider than that of other IL electrolytes but observed in inert working electrodes.<sup>2,18</sup>

To summarize, the incorporation of PYR<sub>13</sub>FSI into PYR<sub>13</sub>TFSI leads to remarkable improvement of the ion transport properties, even at low FSI mole fractions, below its melting point, indicating that properly combining ionic liquid materials hinders the crystallization of the resulting mixture. In particular, the presence of anions (as well as

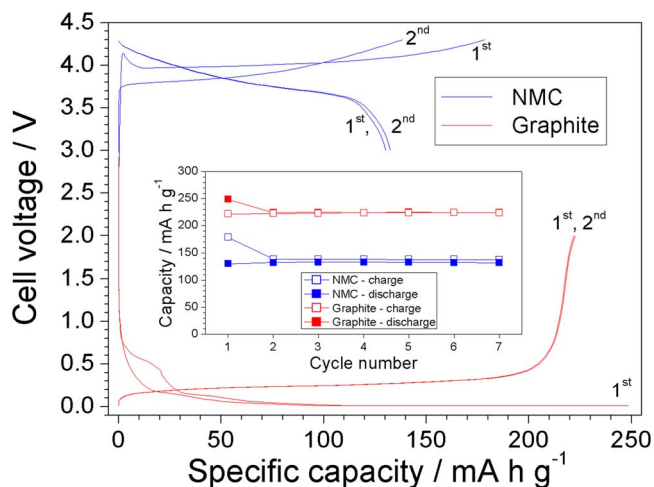


**Figure 9.** Voltage vs. capacity profiles of NMC (blue traces) and graphite (red traces) electrodes in (0.1)LiTFSI-(0.3)PYR<sub>13</sub>TFSI-(0.6)PYR<sub>13</sub>FSI ionic liquid electrolyte. Current rate: 0.1 C. Temperature: 23°C. The insert depicts the initial cycling behavior.

TFSI and FSI) displaying different steric hindrance makes difficult the ion packing through the IL mixtures, which remain in an amorphous phase even at very low temperatures. This interesting effect is due to *ionic confusion*<sup>2,7-9</sup> present in the binary mixtures, shifting the crystallization and, therefore, the melting point to much lower temperatures. Overall, IL blends allow suitably combining/tuning different properties (chemical/electrochemical/thermal stability, film-forming ability, electrode compatibility) in order to obtain ionic liquids with improved characteristics not often achievable by single materials. This allows satisfying different electrode chemistries and/or particular operating conditions. Finally, the LiTFSI mole fraction equal to 0.1 was chosen since it guarantees sufficiently high Li<sup>+</sup> concentration (e.g., above 0.5 M) but, at the same time, falls far with respect to the composition of the solid eutectic<sup>13</sup> (e.g., Li:PYR<sub>13</sub> mole ratio equal to 1:2).

Therefore, the formulation 0.1LiTFSI-0.3PYR<sub>13</sub>TFSI-0.6PYR<sub>13</sub>FSI was selected for the electrolyte to be used in Li/NMC and Li/graphite half-cells, which were subjected to preliminary cycling tests at 0.1 C and 23°C. The results, reported as voltage vs capacity profiles (referred to the initial charge/discharge cycles) in Figure 9, show features typical of NMC<sup>14</sup> (blue traces) and graphite<sup>14</sup> (red traces) electrodes, e.g., plateaus around 4 V (NMC) and below 0.2 V (graphite), respectively, with high reversibility for the Li<sup>+</sup> intercalation process. The plateau observed around 0.5–0.6 V in the Li/graphite first discharge supports for film-forming ability in the 0.1LiTFSI-0.3PYR<sub>13</sub>TFSI-0.6PYR<sub>13</sub>FSI ionic liquid electrolyte. The NMC and graphite electrodes have exhibited reversible capacity of 135 and 220 mA h g<sup>-1</sup>, corresponding to about 87 and 60% of the value recorded in conventional alkyl carbonate-based solutions. The cycling performance, referred to preliminary charge/discharge cycles, is depicted in the insert of Figure 9. A stable capacity value is recorded for both the electrodes, with high coulombic efficiency especially for the graphite anode. This promising behavior indicates feasibility and good compatibility of the 0.1LiTFSI-0.3PYR<sub>13</sub>TFSI-0.6PYR<sub>13</sub>FSI ionic liquid electrolyte with high voltage cathodes and graphite anodes. Work is in progress in our laboratories aimed to deeply investigate the behaviour of these improved LiTFSI-PYR<sub>13</sub>FSI-PYR<sub>13</sub>TFSI electrolyte systems with lithium battery electrodes. The results will be reported in coming soon paper.

### Conclusions

Viable electrolytes, composed by a PYR<sub>13</sub>TFSI/PYR<sub>13</sub>FSI ionic liquid mixture incorporating the LiTFSI salt, for safer, high energy density lithium-ion batteries were properly designed and developed.

The beneficial synergic effect, resulting by blending PYR<sub>13</sub>TFSI and PYR<sub>13</sub>FSI which were then properly combined with LiTFSI, was demonstrated, resulting in improved physicochemical properties with respect to the similar ionic liquid systems.

The 0.1LiTFSI-0.3PYR<sub>13</sub>TFSI-0.6PYR<sub>13</sub>FSI electrolyte formulation has exhibited conductivity approaching 10<sup>-3</sup> S cm<sup>-1</sup> even at -20°C (in good agreement with the rheological properties) in combination with an average electrochemical stability window of 5 V. Preliminary battery tests have shown the feasibility of this ternary electrolyte with high-voltage NMC cathodes and graphite anodes.

### Acknowledgments

The authors wish to acknowledge the EU for funding within the GREENLION Project (FP7 - Contract no 285268).

### References

- H. Ohno Ed., *Electrochemical Aspects of Ionic Liquids*, John Wiley & Sons Inc., Hoboken, New Jersey (2005).
- G. B. Appetecchi, M. Montanino, and S. Passerini, *Ionic Liquid-based Electrolytes for High-Energy Lithium Batteries in Ionic Liquids: Science and Applications*, ACS Symposium Series 1117, A. E. Visser, N. J. Bridges, and R. D. Rogers editors, Oxford University Press, Inc., American Chemical Society, Washington, USA (2013).
- J. R. D. Rogers and K. R. Seddon, *Ionic Liquids: Industrial Application to Green Chemistry (ACS Symposium Series 818)*, American Chemical Society, Washington, USA (2002).
- C. Chiappe and D. Pieraccini, *J. Phys. Org. Chem.*, **18**, 275 (2005).
- F. Castiglione, G. Raos, G. B. Appetecchi, M. Montanino, S. Passerini, M. Moreno, A. Formulari, and A. Mele, *Chem. Chem. Phys.*, **12**, 1784 (2010).
- Q. Zhou, W. A. Henderson, G. B. Appetecchi, and S. Passerini, *J. Phys. Chem. C*, **114**, 6201 (2010).
- M. Montanino, M. Moreno, F. Alessandrini, G. B. Appetecchi, S. Passerini, Q. Zhou, and W. A. Henderson, *Electrochim. Acta*, **60**, 163 (2012).
- O. Miguel, I. Cendoya, G.-T. Kim, N. Löffler, N. Laszczynski, S. Passerini, P. M. Schweizer, F. Castiglione, A. Mele, G. B. Appetecchi, M. Moreno, M. Brandt, T. Kennedy, E. Mullane, K. M. Ryan, M. Olive, and I. de Meatza, *GREENLION Project: Advanced Manufacturing Processes for Low Cost Greener Li-Ion Batteries in Electric Vehicle Batteries: Moving from Research toward Innovation*, Book ID 329226, Springer International Publishing Switzerland (2014).
- G. B. Appetecchi, M. Carewska, M. Montanino, M. Moreno, A. Mele, F. Castiglione, S. V. Meille, G. Raos, and A. Formulari, *Green and Safe Electrolytes Based on Ionic Liquids in Advanced Manufacturing Processes For Low Cost Greener Li-Ion Batteries - The White Paper of The GREENLION Project*, Chapter II, Retrieved from <http://www.greenlionproject.eu> (2016).
- E. Paillard, Q. Zhou, W. A. Henderson, G. B. Appetecchi, M. Montanino, and S. Passerini, *J. Electrochem. Soc.*, **156**, A891 (2009).
- G.-T. Kim, G. B. Appetecchi, M. Montanino, F. Alessandrini, and S. Passerini, *ECS Trans.*, **25**, 127 (2010).
- M. Montanino, F. Alessandrini, S. Passerini, and G. B. Appetecchi, *Electrochim. Acta*, **96**, 124 (2013).
- W. A. Henderson and S. Passerini, *Chem. Mater.*, **16**, 2881 (2004).
- N. Loeffler, J. V. Zamory, N. Laszczynski, I. Doberdo, G.-T. Kim, and S. Passerini, *J. Power Sources*, **248**, 915 (2014).
- J. R. MacDonald, *Impedance Spectroscopy*, John Wiley & Sons Editor, New York, USA (1987).
- B. A. Boukamp, *Solid State Ionics*, **18**, 136 (1986).
- B. A. Boukamp, *Solid State Ionics*, **20**, 31 (1986).
- J. Serra Moreno, Y. Deguchi, S. Panero, B. Scrosati, H. Ohno, E. Simonetti, and G. B. Appetecchi, *Electrochim. Acta*, **191**, 624 (2016).
- I. Nicotera, C. Oliviero, W. A. Henderson, G. B. Appetecchi, and S. Passerini, *J. Phys. Chem. B*, **109**, 22184 (2005).
- D. R. MacFarlane, P. Meakin, J. Sun, N. Amini, and M. Forsyth, *J. Phys. Chem. B*, **103**, 416 (1999).
- I. Bandreš, D. F. Montano, I. Gascofñ, P. Cea, and C. Lafuente, *Electrochim. Acta*, **55**, 2252 (2010).
- W. Xu, E. I. Cooper, and C. A. Angell, *J. Phys. Chem. B*, **107**, 6170 (2003).
- C. A. Angell, W. Xu, M. Yoshizawa, A. Hayashi, and J.-P. Belieres, in: H. Ohno (Ed.), *Ionic Liquids: The Front and Future of Materials Development, High Technology Information*, Tokyo, p.43 (2003).
- D. R. MacFarlane, M. Forsyth, E. I. Izgorodina, A. P. Abbott, G. Annat, and K. Fraser, *Phys. Chem. Chem. Phys.*, **11**, 4962 (2009).
- J. O'M. Bockris and A. K. N. Reddy, *Modern Electrochemistry*, 2nd ed., Plenum Press, New York and London (1998).
- M. Videa, W. Xu, B. Geil, R. Marzke, and C. A. Angell, *J. Electrochem. Soc.*, **148**, A1352 (2001).
- H. Every, A. G. Bishop, M. Forsyth, and D. R. MacFarlane, *Electrochim. Acta*, **45**, 1279 (2000).
- T. Evans, J. Olson, V. Bhat, and S. H. Lee, *J. Power Sources*, **265**, 132 (2014).
- E. Cho, J. Mun, O. B. Chae, O. M. Kwon, H.-T. Kim, J. H. Ryu, Y. G. Kim, and S. M. Oh, *Electrochem. Comm.*, **22**, 1 (2012).